10 GHz Differential Line Modeling of Leadframe-type TQFP Package for High-Speed Serial Interconnection Systems

Seungyoung Ahn, Tae Hong Kim and Joungho Kim

Terahertz Interconnection and Package Laboratory
Department of Electrical Engineering and Computer Science
Korea Advanced Institute of Science and Technology
373-1 Kusong-dong, Yusong-gu, Daejeon 305-701, Korea
Email: javang@eeinfo.kaist.ac.kr
Tel: +82-42-869-8058, Fax: +82-42-869-8058

Abstract

In this paper, we firstly propose differential model of the leadframe type TQFP package. We used 3D full wave simulator to extract 4-port s-parameters. Using optimization method, we finally extracted the spice model parameters. With this extracted spice model, we expected the performance of the package using TDR and eye-diagram simulation.

Introduction

The operational frequencies of digital systems have increased at such a rapid pace over the past few years that nowadays high performance printed circuit boards (PCBs) have to deal with digital signals whose spectral content can reach tens of GHz. To ensure reliable operation at such high data rate, there is a growing tendency to adopt a differential signaling scheme for critical signals. Differential signaling has been important in communications system for more than 50 years, and recent technological advances have pushed analog differential circuit performance limits into RF and low microwave frequencies. Now, it has been a popular choice for multi-gigabit digital applications such as FiberChannel, Infiniband, OIF, RapidIO, Serial-ATA and XAUI, etc. This is because differential signaling has the ability to reject common mode noise such as crosstalk, simultaneous switching noise (SSN), power supply and ground bounce noise.

To support the differential signaling, differential interconnection structure is required. The package system is one of the important parts to guarantee the signal integrity from and to the IC. The differential interconnection in the package level can be supported by ceramic type package, leadframe type package, laminated type package, CSP and so on. Among them, leadframe type TQPF (Thin Quad Flat Pack) package (Fig. 1) is one of the best choices not only because of low cost but also high frequency capability up to 2.5 GHz, thermal dissipation capability up to 2 watts, and 1.2 mm maximum mounted height. To expect the performance of the leadframe type package in signal integrity matters, such as timing margin, slew rate, and inter-symbol interference (ISI), the differential model is currently on demand. However, the electrical model of the leadframe type package for differential signaling is not available yet, and it is necessary to pay attention to the differential signaling characteristics on leadframe type packages.

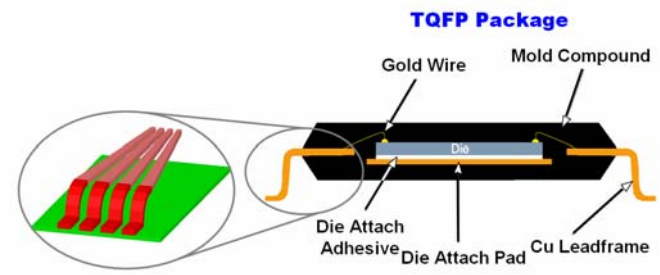

Fig. 1. Cross-sectional structure of TQFP package

Procedure of Model Parameter Extraction

Based on the analysis of 3-D structure of the package, we performed the full-wave simulation using HFSS up to 10 GHz. The complex structures of the leadframe type TQFP package is divided into three parts and simulated individually. Two conductors inside are used as signal lines, and the other two conductor lines outside are used as ground lines (G-S-S-G) as depicted in Fig.2. From the simulated 4-port s-parameters, we calculated 2-port differential s-parameters using following matrix conversion as following [1],[2] as shown in Fig. 2.

$$S_{Mixed\text{-}Mode} = \begin{bmatrix} \begin{bmatrix} S_{11} & S_{12} \\ S_{21} & S_{22} \end{bmatrix}_{DD} & \begin{bmatrix} S_{11} & S_{12} \\ S_{21} & S_{22} \end{bmatrix}_{DC} \\ \begin{bmatrix} S_{11} & S_{12} \\ S_{21} & S_{22} \end{bmatrix}_{CD} & \begin{bmatrix} S_{11} & S_{12} \\ S_{21} & S_{22} \end{bmatrix}_{CC} \end{bmatrix} \quad (1)$$

$$S_{\text{Standard}} = \begin{bmatrix} S_{11} & S_{12} & S_{13} & S_{14} \\ S_{21} & S_{22} & S_{23} & S_{24} \\ S_{31} & S_{32} & S_{33} & S_{34} \\ S_{41} & S_{42} & S_{43} & S_{44} \end{bmatrix} \quad (2)$$

$$S_{\text{Mixed-Mode}} = M \cdot S_{\text{Standard}} \cdot M^{-1} \quad (3)$$

$$M = \frac{1}{\sqrt{2}} \begin{bmatrix} 1 & -1 & 0 & 0 \\ 0 & 0 & 1 & -1 \\ 1 & 1 & 0 & 0 \\ 0 & 0 & 1 & 1 \end{bmatrix} \quad (4)$$

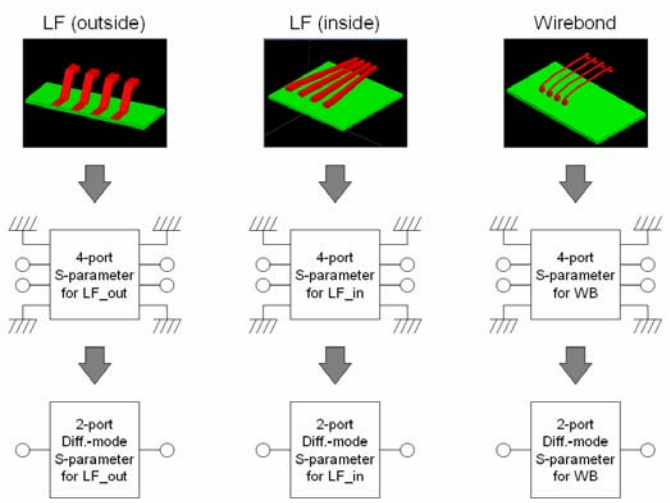

Fig. 2. Procedure to find 2-port differential s-parameters from full-wave simulation using HFSS.

We proposed equivalent circuit model for differential signaling as shown in Fig.3. The differential transmission line is characterized with series inductors and shunt capacitors just like single line because we considered differential-mode signaling only. The resistance of the conductor line was ignored because it didn't affect the s-parameters significantly up to 10 GHz. The lengths of wirebond and leadframe inside mold compound are longer than λ/10 of 10 GHz, we divided the total length into several stages for accuracy of the model parameter extraction.

Proposed equivalent circuit models are compared and optimized to match the differential s-parameters of three parts of the TQFP package simulated using HFSS. Fig. 4 shows the matched s-parameters based on the full-wave simulation and circuit simulation. They show very good correlation between the two s-parameters up to 10 GHz which includes third harmonic frequency of 3 Gbps digital signal.

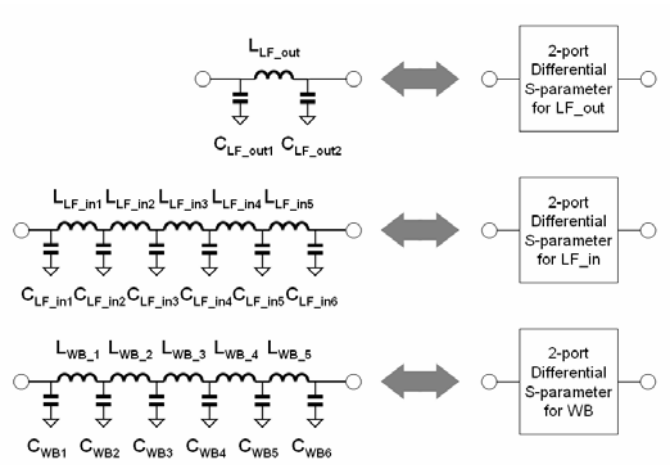

Fig. 3. The equivalent circuit model of the three parts in TQFP package. The optimization is performed through minimization of difference between s-parameters from the circuit model simulation and full-wave simulation. For longer parts of the TQFP package, we divided the interconnection lines into several parts.

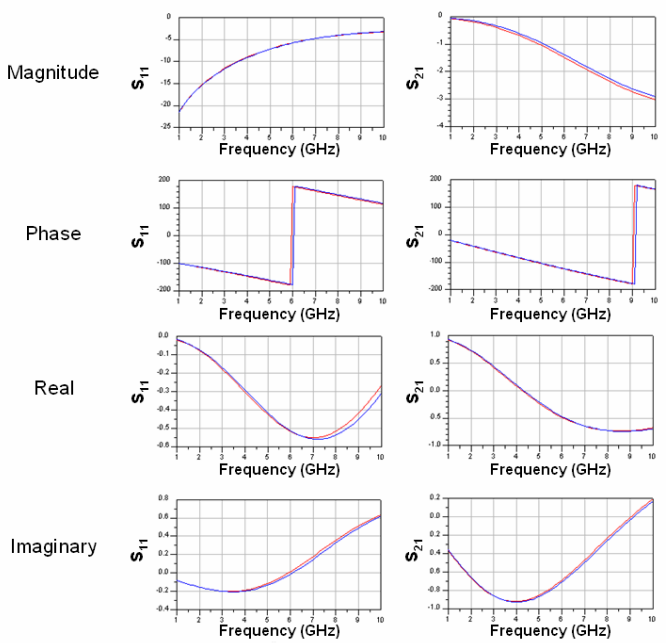

Fig. 4. Matched s-parameters based on full-wave simulation and circuit simulation up to 10 GHz. For full-wave simulation based s-parameters and circuit simulation based s-parameters, are compared. The magnitude, phase, real part, and imaginary part of S_{11} and S_{21} are compared.

The extracted spice model parameters are shown in Fig. 5. Using these parameters we simulated time-domain reflection (TDR) and eye-diagram simulation.

Before the simulation, we can expect the result of the simulation from the total inductance and capacitance, we can expect the impedance profile The leadframe outside (LF_out) has higher inductance and the impedance of the wirebond is more inductive than leadframe inside mold compound.

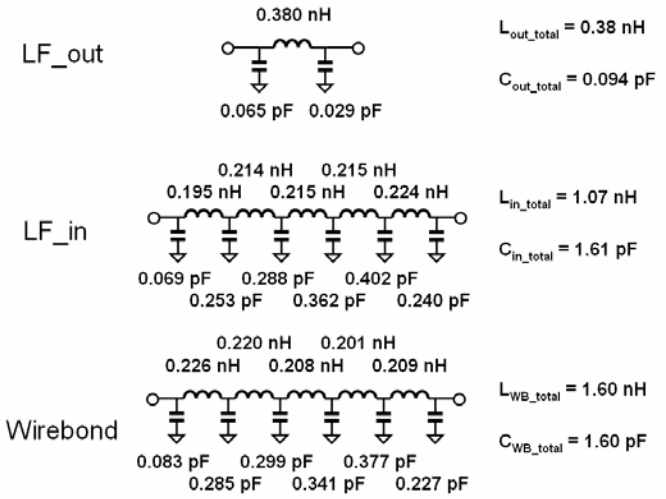

Fig. 5. The extracted equivalent circuit model parameters leadframe (outside), leadframe (inside) and wirebond. TQFP package. All the parameters are valid only in differential-mode signaling.

The complete procedure of the model parameter extraction is summarized in Fig. 6.

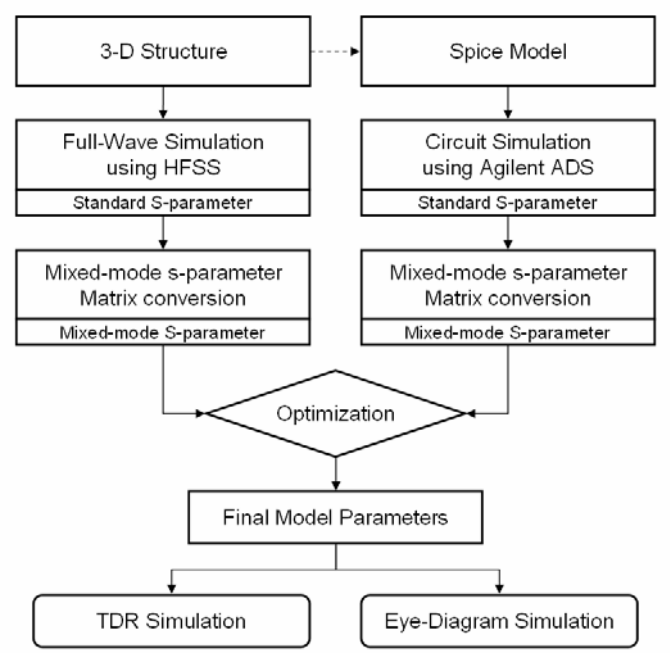

Fig. 6. Procedure of model parameter extraction. From the 3-D structure of package, s-parameters based on full-wave FEM simulation and equivalent circuit simulations are used for optimization. The TDR simulation and eye-diagram simulation is performed with the extracted model parameters.

Verification using TDR and Eye-diagram Simulation

Fig. 7 shows the simulated TDR waveform of the TQFP package including the input capacitance of the IC when the input signal has 30 ps of risetime. The lower peak shows capacitive effect and upper peak shows the inductive effect. The interconnection line is terminated with 2 pF capacitance and matched resistance

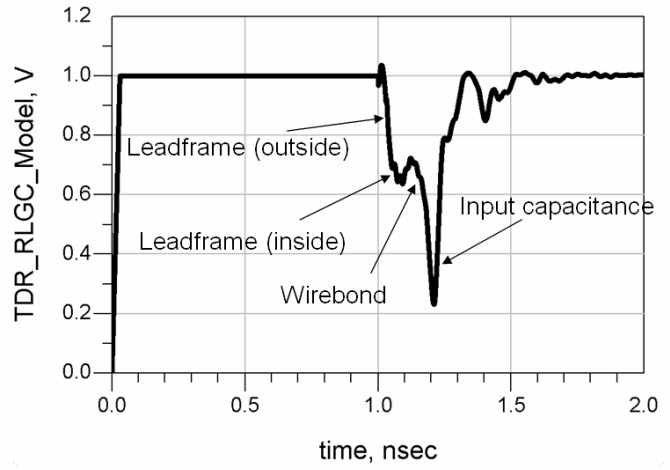

Fig. 7. TDR waveform simulated using extracted model parameters. The effect of input capacitance is the most significant in this structure.

According to TDR simulation results, the leadframe structure and input capacitance of the IC affect the waveform significantly. When the length of the leadframe increases, the impedance mismatch of the leadframe happens consequently. In that case, the design of the leadframe structure differential interconnection becomes very important in the view of the impedance matching between PCB trace and leadframe to improve signal integrity. The inductance of the wirebond affects the TDR waveform seriously when the length of the wirebond increases. The unwanted peak of the TDR waveform comes from high impedance of the inductive wirebond structure. However, if the pitch of the leadframe conductor lines are small enough to result in capacitance to make lower peak on TDR waveform, or if the input capacitance of the IC is necessary to prevent the electro static discharge (ESD) problem, we can utilize the inductive effect of wirebond to reduce the lower peak of TDR waveform by increasing the inductance.

Also, we have simulated the whole system in time-domain including leadframe package, two 20cm-long lossy PCB transmission lines, connectors, and 30cm-long cable to estimate eye-diagram in real measurement system. In the eye-diagram simulations, the waveform at the receiver is taken as a waveform at Rx probing point of the real measurement system as shown in Fig. 8.

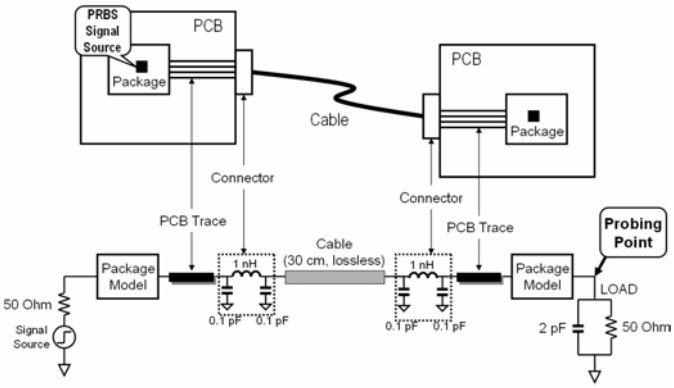

Fig. 8. Setup for time-domain eye-simulation.

Fig. 9 shows the eye-diagram waveforms simulated with 127-bit NRZ (a) 1.5 Gbps and (b) 3 Gbps pseudo random bit sequence (PRBS) signal source. With the large effect of the lossy PCB lines with loss tangent of 0.03, the eye of simulation is small due to the signal degradation, even though the leadframe type TQFP package can guarantee up to 3 GHz.

The eye-diagrams of the spice model with different inductances of wirebond are compared while the other conditions are the same. As the impedance of the TQFP package is smaller than that of the signal line on PCB or cable, the increase of the inductance improved eye-diagram in jitter and rise time as shown in Fig. 10 (a) and (b).

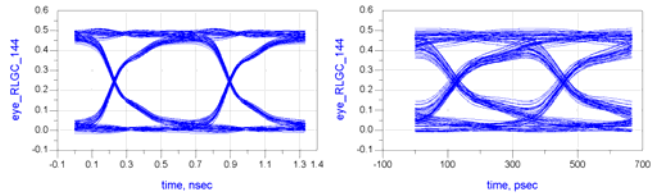

(a) 1.5 Gbps (b) 3 Gbps

Fig. 9. Eye-diagram waveforms with the change of operation frequency.

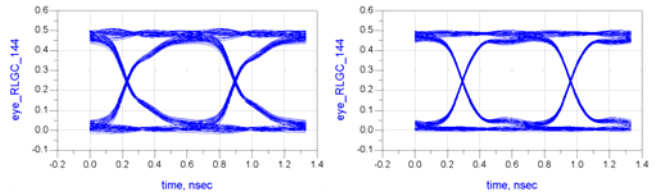

(a) L_{WB_total} = 0.16 nH (b) L_{WB_total} = 0.48 nH

Fig. 10. Eye-diagram waveforms with the change of inductance of wirebond.

Conclusions

Differential model of the leadframe type TQFP package is proposed and the spice model parameters are extracted using 3D full-wave simulation. Based on the extracted equivalent circuit model, time-domain reflection and eye-diagram simulations are performed. With this modeling and simulation method, we can expect the high-frequency characteristic and performance at the simulation stage before the fabrication.

References

[1] David E. Bockelman and William R. Eisenstadt, "Combined Differential and Common-Mode Scattering Parameters: Theory and Simulation," *IEEE Transaction on Microwave Theory and Techniques*, Vol. MTT-43, pp. 1530-1539, 1995.

[2] Garth Sundberg, "Understanding Single-Ended and Mixed-Mode S-parameters," *Microwaves & RF*, pp. 121-128, 2001.